ELSEVIER

Contents lists available at ScienceDirect

# **Environmental Research**

journal homepage: www.elsevier.com/locate/envres





# Core taxa, co-occurrence pattern, diversity, and metabolic pathways contributing to robust anaerobic biodegradation of chlorophenol

Ming Lin <sup>a,d</sup>, Chenhui Pan <sup>a,d</sup>, Chenyi Qian <sup>a,d</sup>, Fei Tang <sup>a,d</sup>, Siwen Zhao <sup>a,d</sup>, Jun Guo <sup>a,c</sup>, Yongming Zhang <sup>a,d</sup>, Jiaxiu Song <sup>a,d,\*</sup>, Bruce E. Rittmann <sup>b</sup>

- <sup>a</sup> School of Environmental and Geographical Sciences, Shanghai Normal University, Shanghai, 200234, PR China
- <sup>b</sup> Biodesign Swette Center for Environmental Biotechnology, Arizona State University, Tempe, AZ, 85287-5701, USA
- <sup>c</sup> Department of Environmental Science and Engineering, Fudan University, Shanghai, 200238, PR China
- d Yangtze River Delta Urban Wetland Ecosystem National Field Scientific Observation and Research Station, Shanghai, 200234, PR China

### ARTICLE INFO

Handling editor: Aijie Wang

Keywords: Robustness Trichlorophenol Co-occurrence network Diversity Dechlorination Microbiome

## ABSTRACT

It is hard to achieve robustness in anaerobic biodegradation of trichlorophenol (TCP). We hypothesized that specific combinations of environmental factors determine phylogenetic diversity and play important roles in the decomposition and stability of TCP-biodegrading bacteria. The anaerobic bioreactor was operated at 35 °C (H condition) or 30  $^{\circ}$ C (L condition) and mainly fed with TCP (from 28  $\mu M$  to 180  $\mu M$ ) and organic material. Metagenome sequencing was combined with 16S rRNA gene amplicon sequencing for the microbial community analysis. The results exhibited that the property of robustness occurred in specific conditions. The corresponding co-occurrence and diversity patterns suggest high collectivization, degree and evenness for robust communities. Two types of core functional taxa were recognized: dechlorinators (unclassified Anaerolineae, Thermanaerothrix and Desulfovibrio) and ring-opening members (unclassified Proteobacteria, Methanosarcina, Methanoperedens, and Rubrobacter). The deterministic process of the expansion of niche of syntrophic bacteria at higher temperatures was confirmed. The reductive and hydrolytic dechlorination mechanisms jointly lead to C-Cl bond cleavage. H ultimately adapted to the stress of high TCP loading, with more abundant ring-opening enzyme (EC 3.1.1.45, ~55%) and hydrolytic dechlorinase (EC 3.8.1.5, 26.5%) genes than L (~47%, 10.5%). The functional structure (based on KEGG) in H was highly stable despite the high loading of TCP (up to 60 μM), but not in L. Furthermore, an unknown taxon with multiple functions (dechlorinating and ring-opening) was found based on genetic sequencing; its functional contribution of EC 3.8.1.5 in H (26.5%) was higher than that in L (10.5%), and it possessed a new metabolic pathway for biodegradation of halogenated aromatic compounds. This new finding is supplementary to the robust mechanisms underlying organic chlorine biodegradation, which can be used to support the engineering, regulation, and design of synthetic microbiomes.

Funding: This work was supported by the National Natural Science Foundation of China (No. 21677100); the Natural Science Foundation of Shanghai (23ZR1446900); and the Fundamental Research Funds for the Central Universities (No. B210204007) and PAPD.

# 1. Introduction

Chlorophenols (CPs) have attracted significant attention as relatively recalcitrant priority pollutants (EPA, 2015; Hou et al., 2022; Kravos et al., 2022; Lin et al., 2019; Yang et al., 2020). Owing to its strong

electronegativity and resistance to oxidative cleavage, anaerobic dechlorination is more effective for biodegrading CPs (Diaz-Baez and Valderrama-Rincon., 2017; Ali et al., 2020; Limam et al., 2016). The anaerobic degradation of CPs relies on task specialization and resource exchange of diverse microbial communities, as well as other intrinsic trade-offs, to reduce the metabolic burden (Qi et al., 2021)and achieve mineralization. Owing to the toxicity of CPs and inefficient community collaboration, the efficiency and stability of self-assembled CP-degrading microbiota are compromised (Lucas et al., 2018; Rittmann and McCarty, 2012; Yang and Speece, 1986). Therefore, characterizing the

E-mail address: songjiaxiu@shnu.edu.cn (J. Song).

<sup>\*</sup> Corresponding author. School of Environmental and Geographical Sciences, Shanghai Normal University, No. 100 Guilin Road, Shanghai, 200234, shanghai, PR China.

long-term degradation, functional evolution, and stability of microbial communities, along with identifying core members, microbial interactions, and metabolic pathways, is crucial for an in-depth understanding of community construction and maintenance mechanisms.

The key function—dechlorination can be enhanced through "adaptation" of active sludge community (Rittmann and McCarty, 2012; Yang and Speece, 1986). Recent studies have indicated the coexistence of reductive and hydrolytic dechlorination in anaerobic system (Chen et al., 2021; Temme et al., 2019). Similar to typical species of anaerobic reduction dechlorination, Dehalococcoidia (Adrian et al., 2000; Jugder et al., 2016; Payne et al., 2019; Kaya et al., 2019; Kruse et al., 2021; Yan et al., 2021; Assadi et al., 2021) and common taxa (e.g., Desulfomonile, Desulfovibrio, Desulfitobacterium) (Lin et al., 2019; Diaz-Baez and Valderrama-Rincon, 2017; Adrenz and Loffler, 2016) found that receiving CPs grew best in mixed microbial consortia, relying on non-dechlorinating members to provide H<sub>2</sub> as an electron donor, along with essential micronutrients (Juteau et al., 1995; Zheng et al., 2021; Hug et al., 2012). These bacteria dechlorinate through reductive organohalide respiration. For example, the pathway for 2,4,6-trichlorophenol (TCP)is TCP→ 2,4-DCP→ 4-CP→ phenol, which then can be converted to catechol and benzoate by mixed anaerobic microbial consortia whose structure and function have not been characterized (Mikesell and Boyd, 1986; Ghattas et al., 2017). Furthermore, previous studies have shown that the rearrangement of the catalytic residues of hydrolytic dichlorination enzymes (e.g., haloalkane dehalogenases and L-2-haloacid dehalogenase) predates the industrial revolution (Hasan et al., 2011; Jesenska et al., 2009; Li and Shao, 2014; Chovancova et al., 2007; Chmelova et al., 2020), suggesting that hydrolytic dechlorination has a common metabolic capability in nature. These enzymes have been studied predominantly in aerobic environments; however, recent evidence indicates that their abundance increases when the environment is enriched with high concentrations of organic chlorine (Chen et al., 2021; Temme et al., 2019). It is currently unknown whether hydrolytic dehalogenases are active, and how they interact with reduction dechlorination during CPs degradation.

Complete degradation requires the participation of microbial taxa in enzymes that can open ring structures. Further degradation of 4-CP proceeds via ring-cleavage pathways (Konovalova et al., 2009; Nordin et al., 2005; Solyanikova and Golovleva, 2004, 2011; Gaytan et al., 2020; Semenova et al., 2022; Singh et al., 2018). Song et al. (2019) found that 38 °C led to higher TCP degradation efficiency in batch anaerobic system than lower temperature (30 °C). This can be attributed to the high abundances of Syntrophobacter (Syntrophy) and Ignavibacterium (degrading aromatic hydrocarbons), which facilitate cross-feeding between strains and promote complete degradation metabolism. It is not clear whether this rule also consisted to continuous flow conditions (Assadi et al., 2021; Song et al., 2019; Delgado et al., 2017; Li et al., 2019; Mortan et al., 2017; Patel et al., 2022). Additionally, some studies have shown that hydrolytic dechlorination is positively correlated with temperature (Xi et al., 2015). According to the latest research, the selection process of the active sludge system is obviously more advantageous than ecological drift due to the very high cell density and "specific" function (Vanwonterghem et al., 2016; Yu et al., 2021). Therefore, ecological interactions can be accurately inferred using environmental gradients (Sun et al., 2021), which are of great significance (Gralka et al., 2020) for promoting the biotransformation of CPs.

In summary, we propose the research assumption that a specific combination of environmental factors (temperature and TCP loading) determines the phylogenetic diversity, as well as the decomposition and stability of TCP-biodegrading community. In this study, we operated two upflow anaerobic bioreactors under high- and low-temperature conditions. Both reactors were continuously fed with TCP, non-chlorinated organic substrates, and essential nutrients. Their performances, communities, and metabolic pathways were characterized. The core members, auxiliary members, and their interactions in the

communities were identified. This study proposes new pathways for TCP degradation that are promising for understanding the mechanisms, predictions, and operations of the collaborative biodegradation of various contaminants.

### 2. Materials and methods

#### 2.1. Reactor operations

As shown in Fig. S1, the two up-flow anaerobic sludge blanket reactors were operated in parallel. The inoculum was collected from a secondary sedimentation tank at Shanghai Changqiao Sewage Treatment Plant. The sludge was inoculated into each reactor at the same volume (0.5 L). The influent was a synthetic medium composed of lactic acid, TCP, vitamins, and trace elements as described by Song et al. (2019) Feed water was pumped into the reactor using a peristaltic pump. TCP concentration in industrial wastewater is commonly 10-200 µ M, and can reach higher concentrations in accident leakage. The TCP concentrations in the study were increased stepwise over five phases: I (28  $\pm$  2  $\mu M$ ), II (50  $\pm$  5  $\mu M$ ), III (70  $\pm$  5  $\mu M$ ), IV (120  $\pm$  10  $\mu M$ ), and V (180  $\pm$  10  $\mu$ M). Sodium lactate was used as the electron donor at 10 mM. Microbial samples were taken regularly, frozen rapidly in a −40 °C freezer, and subsequently subjected to DNA extraction and high-throughput sequencing. The two reactors used the same HRT, with 26 h for 1-548d and 52 h thereafter.

## 2.2. Chemicals and analytical methods

Reference materials of TCP, DCP, 4CP, phenol (Dr.Ehrenstorfer, GER) were purchased from Shanghai Titan Technology Co., Ltd. COD was measured using a complete set of reagents (Hash, US).

TCP and its intermediates (DCP, 4CP, phenol) were analyzed on a high performance liquid chromatograph (ThemoFisher Ultimate 3000, US) with a 250 nm UV absorbance meter. The CP determination column used was an Agilent 5HC-C18 (2) 150 mm  $\times$  4.6 mm column with a mobile phase of methanol: water (containing 1% acetic acid) at 80:20 (v/v), flow rate 1.00 mL/min, detection wavelength 282 nm, a detection temperature of 25  $^{\circ}$ C, and injection volume 10  $\mu$ L. COD was determined by using the potassium dichromate method and fast analyzer (Hash DRB200 and DR3900, US). All the test samples were passed through a 0.22  $\mu$ m water filter and then assayed.

# 2.3. 16S rDNA gene sequencing and analysis

High-throughput sequencing was performed by Shanghai Majorbio Pharm Technology Co., Ltd. Details of all the analysis methods are provided in the SI. The sequencing process included DNA extraction, primer design, primer connector synthesis, polymerase chain reaction (PCR) amplification, product purification, fluorescence quantification, construction of a MiSeq PE library, and MiSeq sequencing. After DNA was extracted, the DNA was broken into fragments of approximately 400-bp fragments for double-ended sequencing (Covaris M220), construction of a PE library with recycled RCR products (NEXTFLEX Rapid DNA-Seq Kit), amplification of DNA clusters by bridge PCR (NovaSeq Reagent Kits/HiSeq X Reagent Kits), and sequencing (Illumina NovaSeq/Hiseq Xten). the online platform Majorbio Cloud Platform (Ren et al., 2022). The raw datasets of 16S rDNA gene sequencing datasets were deposited in NCBI as public data with the accession number SRP374461.

# 2.4. Metagenome sequencing and analysis

After DNA was extracted, the DNA was broken into  $\sim$ 400-bp fragments for double-ended sequencing (Covaris M220), construction of a PE library with recycled RCR products (NEXTFLEX Rapid DNA-Seq Kit), amplification of DNA clusters by bridge PCR (NovaSeq Reagent Kits/HiSeq X Reagent Kits), and sequencing (Illumina NovaSeq/Hiseq Xten).

Details of all the analysis methods are provided in the SI. The raw metagenome sequencing datasets were deposited in NCBI as public data with accession number SRP374461.

### 3. Results and discussion

#### 3.1. Reactor performance

The reactor performance is shown in Fig. 1. It exhibited that stable and efficient performance occurred under L (low TCP loading) and H (high TCP loading) conditions.

After a disorderly start-up phase, the indicators tended to stabilize based on the observations of COD removal. In phases I and II, L and H achieved similar COD removal efficiencies, with >95% removal of the influent COD. For the CPs, the performance was better in L than in H: effluent CP concentrations of 0.4–8.1  $\mu M$  for L and 6.2–18  $\mu M$  for H. With a higher TCP-loading in phase III (days 260-419), H continued to show good performance stability (COD removal close to 95%), but L began to show erratic COD removal (50-70%) and the accumulation of 4-CP, as high as 62 μM. After a long period of time, some recovery was observed at the end of this phase. At the beginning of phase IV (days 420-626), both reactors experienced instability, although H was significantly less affected than was L. Although the H effluent transitorily contained TCP (8.1 μM), other phenols still were rarely detected. In contrast, the effluent of L contained substantial phenol and 4-CP, around  $60 \mu M$ . The increase in hydraulic retention time on day 555 led to a significant recovery in the performance of H, but not L. In phase V (days 627–670), the performance of the two reactors deteriorated significantly due to the still higher input concentration of TCP (180 µM). However, the performance of H improved over time, while the performance of L continually deteriorated, eventually leading to a 4-CP concentration of  $120~\mu M$ , as well as incomplete removals of TCP and DCP.

# 3.2. Abundant species and structures by 16S rDNA gene-sequencing

The microbial diversity obtained by 16S rDNA gene sequencing is shown in Fig. 2a (genus level) and Fig. S2 (class-level). LEfSe analysis (LDA score >3.5) was used to compare species differences and to identify potential core species in the late stages (Fig. S3). Canonical Correspondence Analysis (CCA) was used to rank the importance of these potential core species (Fig. 2b).

Overall, with increasing TCP loading, the climax community patterns in both systems exhibited continuous variations. According to LEfse and CCA analyses, the potential core species with high abundance were Thermodesulfovibrionia (Tdb, in L), *Syntrophbacter* (in H), *Unclassified* Anaerolineae (in H), *Desulfovibrio* (in L), and SBR1031 (in H).

Tdb was a key taxon in both reactors (average abundance of 25% in H and 37% in L). Tdb has been associated with stimulation of methanogen growth,  $CH_4$  generation, and reducing sulfate (Bai et al., 2022; He et al., 2021). Tdb was found in a system undergoing long-term CP stress but did not show dechlorination. The lack of dechlorination by Tdb might explain the relatively low dechlorination efficiency of L (Wang et al., 2021).

The second most abundant taxon in H was *Syntrophobacter* (17% in RL and 4% in RL), belonging to the class Syntrophobacteria (class 17%). It is generally believed that *Syntrophobacter* can ferment organic matter to produce H<sub>2</sub>, which is an electron donor in reductive dechlorination (Wang et al., 2021; Li et al., 2018; Mai and Stuckey, 2018; Wu et al., 2021). Higher temperatures may have contributed to the relatively higher abundance of *Syntrophobacter* in H (Song et al., 2019).

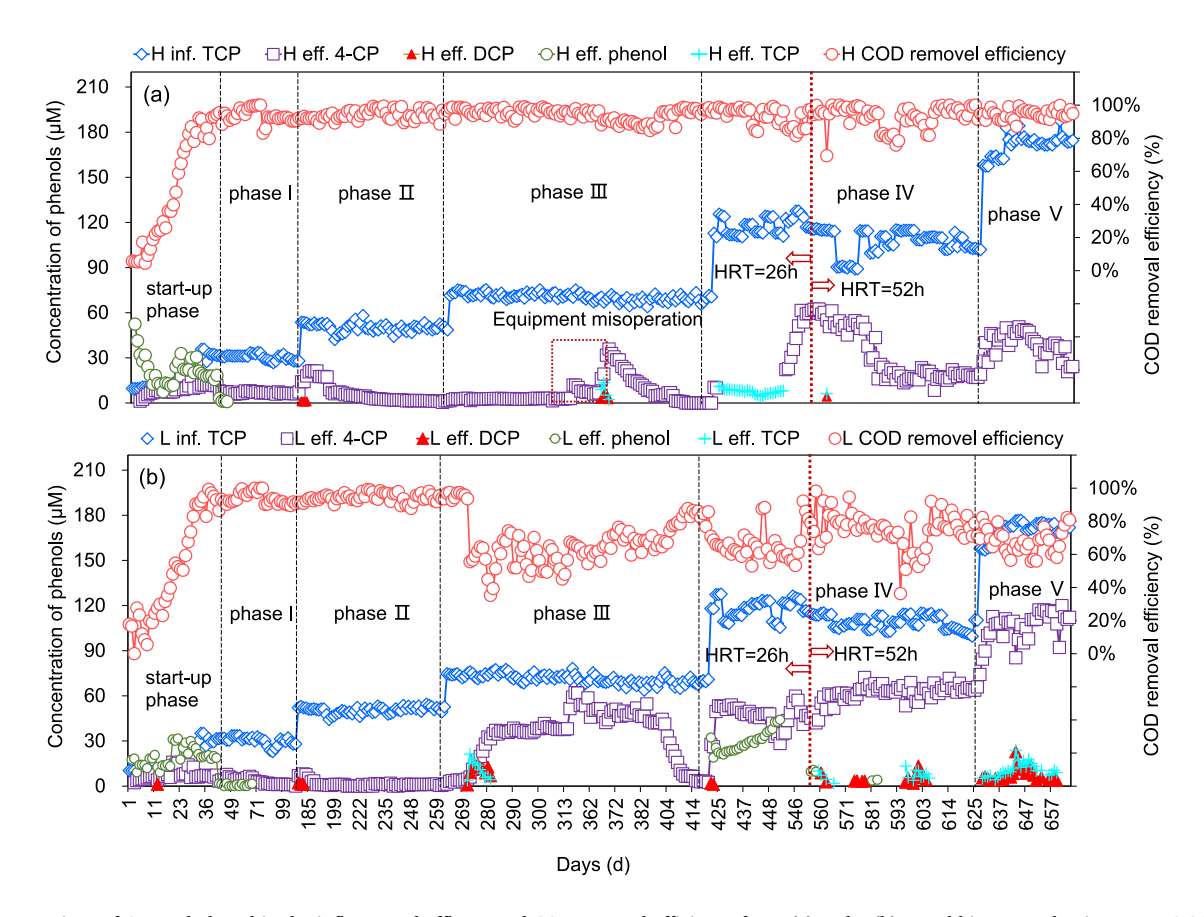
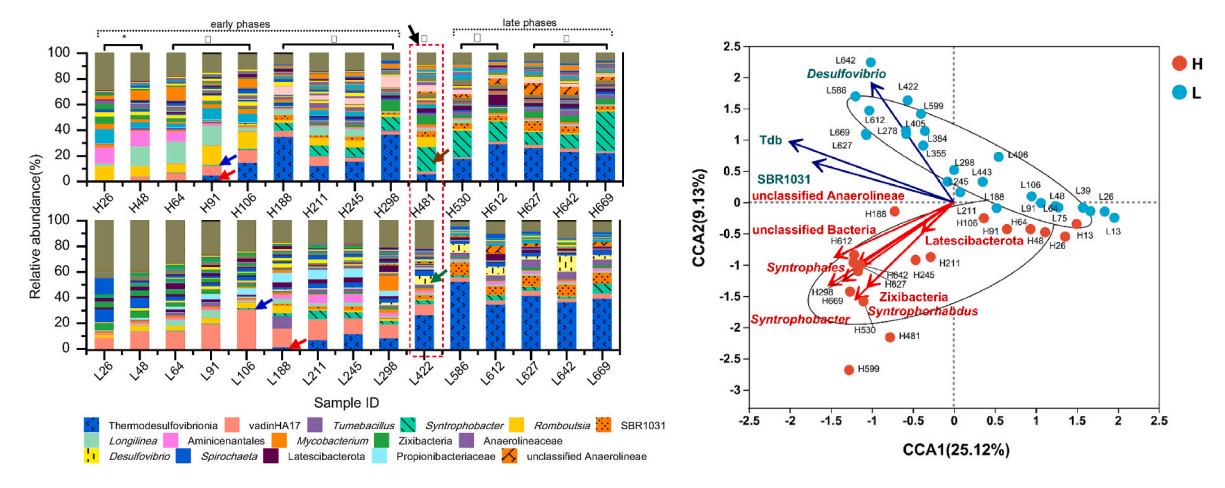


Fig. 1. Concentrations of CPs and phenol in the influent and effluent and COD removel efficiency for H (a) and L (b). Total biogas productions were 0.31 and 0.24 m $^3$ /kg COD for H and L, respectively.



**Fig. 2.** (a) Relative abundances at the genus level during community evolution. The numbers after H and L are running days. The blue arrows indicate *Syntrophobacter* to appear; the red arrows indicate Tdb to appear. The brown arrows indicates that *Syntrophobacter* started to expand in H; the green arrow indicates that *Desulfovibrio* started to expand in L. \*means start-up phase. (b) Canonical correspondence analysis of potential core species. The arrows in the figure represent different species, and the length of the arrow indicates the importance of that species. The acute angle between two arrows indicates a positive correlation with two species, while the obtuse angle signifies a negative correlation.

Another abundant taxon in L was *Desulfovibrio* (genus: 6.1% in L but only 0.39% in H). Many studies have shown that its abundance increases in environments containing chlorinated organics and that it can remove

chlorine atoms through extracellular respiration (Anam et al., 2019; Chattopadhyay et al., 2022). Given that *Desulfovibrio* has exhibited enrichment at lower temperatures (Song et al., 2019), it is speculated

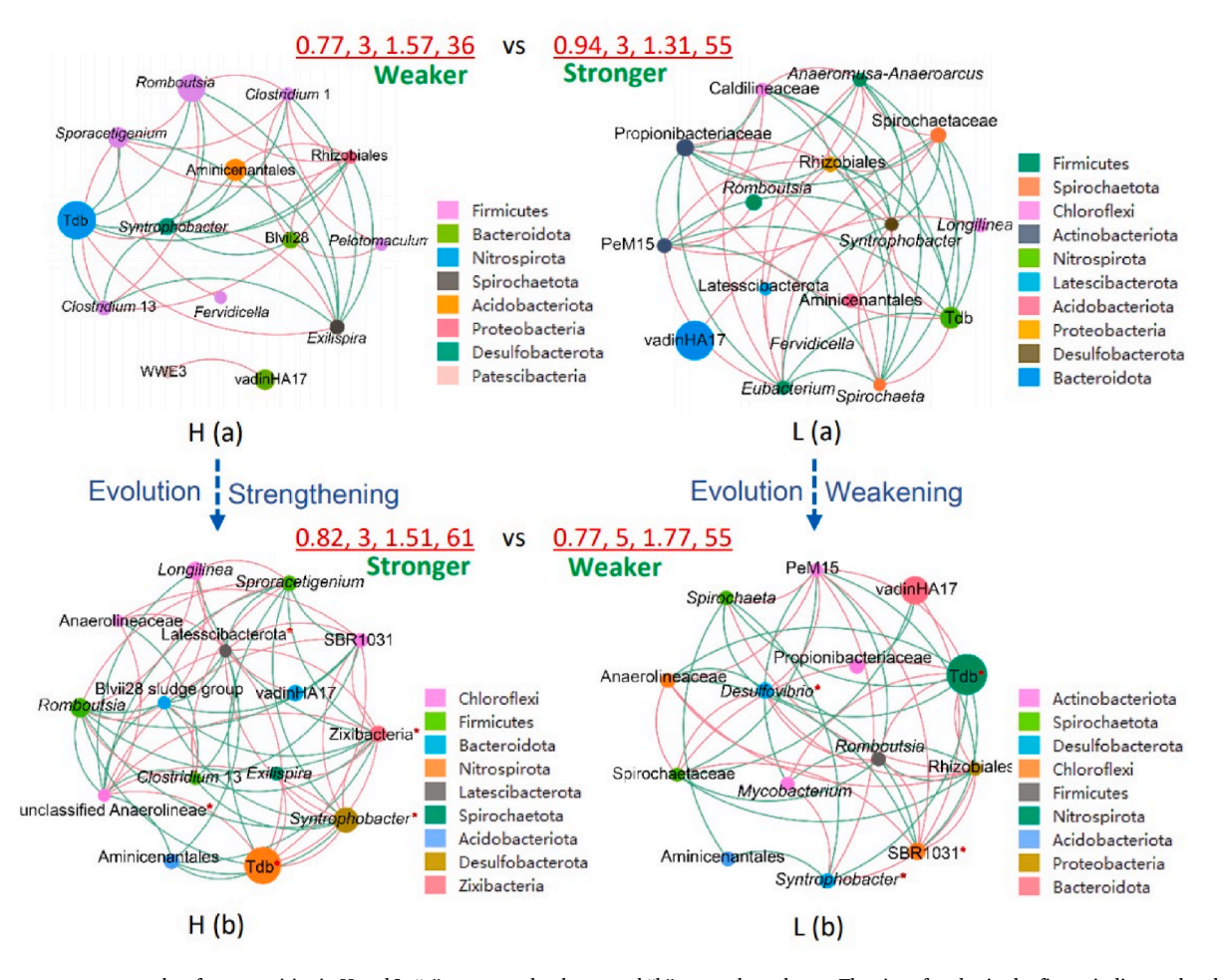


Fig. 3. Co-occurrence networks of communities in H and L, "a" means early phases and "b" means late phases. The size of nodes in the figure indicates the abundance of species, and colors indicate different Phyla. The colors of the edges (lines) represent positive and negative correlations: a pink color represents a positive correlation, and a green color represents a negative correlation. The four red numbers near each network graph represent the Clustering Coefficient, Diameter, Average Shortest Path Length and number of Edges, respectively (from left to right). The blue dashed arrow represents the directions of evolution.

that high content of *Desulfovibrio* in L would be the result of environmental selection.

Anaerolineae, a member of Chloroflexi, had similar abundances in both systems:21% in H and 24% in L. Its phylogenetic location was on the branch of a tree with *Dhc* and other species known to conduct reductive dechlorination (Yang et al., 2020). This microbial taxon is often found in anaerobic systems, including those exposed to organochlorine compounds (Matturro et al., 2016; Zerva et al., 2021). Unclassified Anaerolineae in H and SBR1031 in L, the two species with the highest abundance among Anaerolineae, have not been reported to be dechlorinators before.

It is noteworthy that the syntrophic taxa (*Syntrophobacter*, *Syntropicorhabdus*, and *Syntropicales*) were gradually enriched in H with high proportions and diversity, and strengthened syntrophy. Comparing these findings with those of a previous work (Song et al., 2019), despite different cultivation methods and seed sludges, the preference for syntrophic species was consistent with these results. The behavior of these species can follow a repeatable trajectory under specific conditions.

# 3.3. Co-occurrence networks of communities

The connectivity patterns of the abundant taxa (top 15, Fig. 3 and Table S1) in early and late phases were obtained to determine the core species by calculating the Spearman correlation coefficient (R  $\geq$  0.6, P < 0.05).

Efficient microbiomes often consist of small-world networks (Kulikova and Perminova, 2021; Watts and Strogatz, 1998), which have small characteristic path lengths and large clustering coefficients. According to Fig. 3 and Table S1, both systems are small-world networks. L of the early phases and H of the late phase had a higher Average Cluster Coefficient, lower diameter, shorter Average Path Lengths and more Edges, indicating a higher degree of clustering of core species with robust function. This demonstrates the significance of the community network structure, which corroborates that higher connectivity, a more compact community structure, and greater collectivization could be beneficial attribute (Saleem et al., 2019). According to the network coefficients (Table S1), we reiterated that the taxa mentioned above —Tdb, Syntrophbacter, Unclassified Anaerolineae, Desulfovibrio and SBR1031-were core taxa because of their high network degree and clustering coefficient in the community nodes. The significance of Zixibacteria and Latescibacterota, which exhibited exceptionally high network coefficients, is also highlighted. A study of the Earth's microbial co-occurrence network reported that Latescibacterota is present in specialist hubs in a wide range of habitats and is considered an important and widespread hub species (Coskun et al., 2019). Zixibacteria (Gao and Wang, 2007), a relatively understudied microbiota, poses challenges for cultivation, but harbors highly functional genes related to iron redox metabolism. These two species are postulated to be potential dechlorinating species (Iasakov et al., 2022; Kapoor et al., 2021) or core taxa according to their identification in CCA (Fig. 2b). The importance of Zixibacteria was significant because the arrow was considerably long.

# 3.4. Diversity characteristics during community evolution

PCoA was performed using the unweighted UniFrac distance algorithm. Fig. 4 shows that the H community separated from the L community along the PC2 axis. This demonstrated that temperature frames the community structure. Each group moved chronologically from left to right along the PC1 axis. The two communities were more similar along the PC2 axis in the early phases (I and II), when both systems had similar and good performances. The communities then gradually separated after about day 260 (phases III), when the higher input of TCP (70  $\mu m$ ) lead to much more significantly deteriorated performance in L. The distance along the PC2 axis increased dramatically in phases III – V. Although the communities were separated in the early phases based on the temperature, both communities evolved in similar patterns (Fig. 2a). In

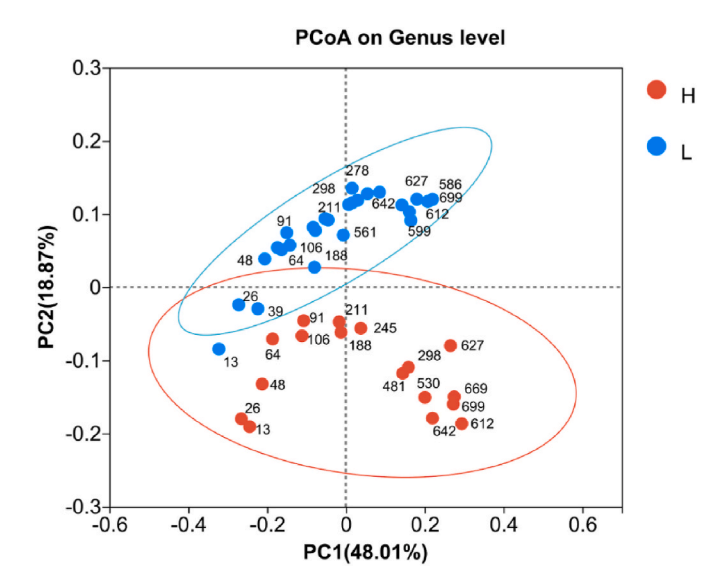


Fig. 4. PCoA analysis (unweighted unifrac) on genus level in which the numbers are the running days. The ellipses are the confidence intervals (95%).

particular, core taxa—Tdb, Anaerolineae, *Syntrophobacter* with high TCP stress tolerance—began to emerge and gradually expanded their *niches* over time.

As shown in Fig. 5a, in the early phases, the community in H exhibited higher Shannon and Simpson indices but lower Simpsoneven and functional levels than in L. In the late phases (Fig. 5b), the community in L had a higher Chao and Simpson index, a lower Simpson index, and higher efficiency and stability than that in H. These results indicate the importance of community evenness. The communities in both L (early phase) and H (late phase) formed a multi-dominant population distribution pattern (high evenness and low ecological dominance), which may facilitate better division of labor and resource allocation, resulting in higher functional levels. Conversely, when the community exhibited a single-dominant pattern (low evenness and high ecological dominance), efficiency and stability decreased accordingly.

# 3.5. Genes, functional contributions, and metabolic pathways

Based on their 16S rRNA gene sequences, the samples were screened using MicoPITA for genes encoding key functional genes; changing trends and correlation analysis of key genes and TCP amount are shown in Fig. 6. A comparison of these differences is shown in Fig. 7a. The NR species (subset) annotated to the enzymes and the average value of the functional contribution of the enzymes in the late phases are summarized in Fig. 7b for further identification of the core species. The profile of the assembly process was illustrated by the dynamics of the functional contributions of the species (Fig. S4). The functional structure (based on KEGG) in H was highly stable despite the high loading of TCP, but not in L. Fig. 8 integrates all the information into the TCP metabolic pathways that require the coordinated action of several different microorganisms, similar to lindane biodegradation.

As shown in Fig. 6, the genes EC 3.1.1.45 (in H & L) and EC 3.8.1.5 (in H) exhibited a strong positive correlation with TCP loading throughout the process, indicating the role of core metabolic pathways in the stable biodegradation of TCP. On the other hand, the genes EC 3.8.1.5 (in L), EC 3.8.1.2 and EC 1.3.11.2 (in H & L) show a significant positive correlation with low TCP loadings (<70  $\mu$ M) following by a significant decline, suggesting their intolerance to high TCP loadings. However, due to the interaction between the substrates and the genes, the TCP abundance of all functional genes either ceased to increase or decreased after reaching to 70  $\mu$ M. This finding is consistent with the drastic changes observed in community patterns (Fig. 2a) and PCoA

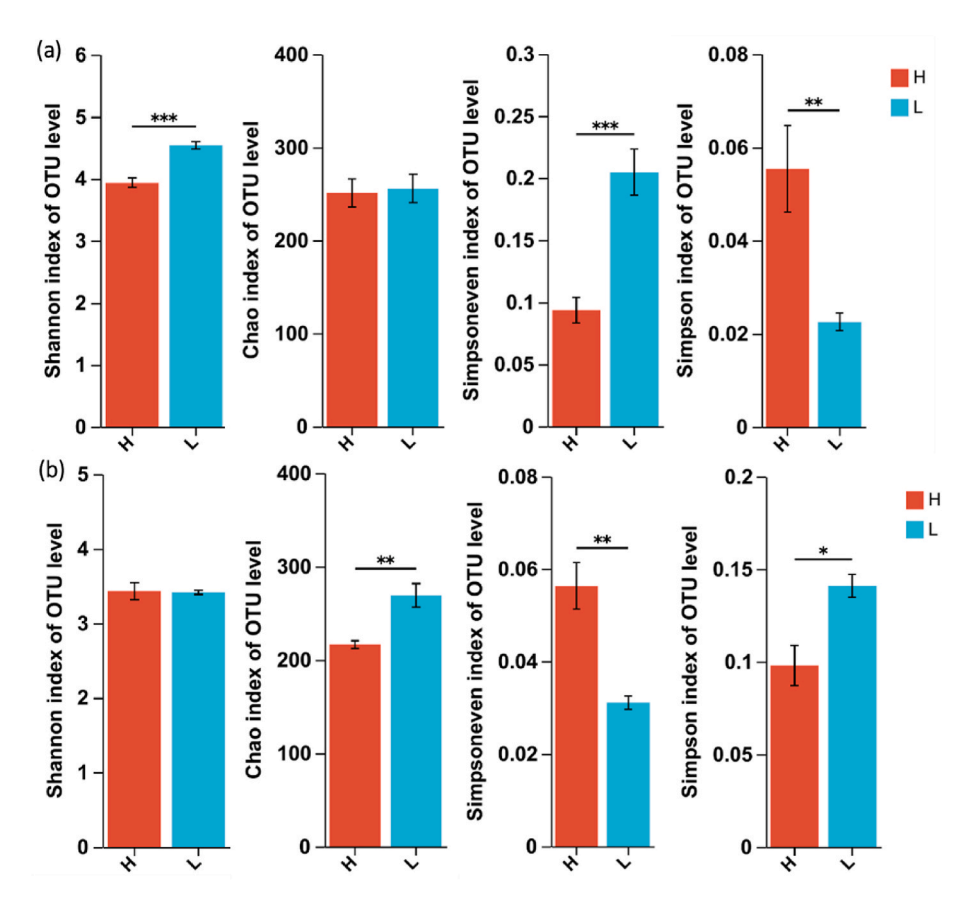
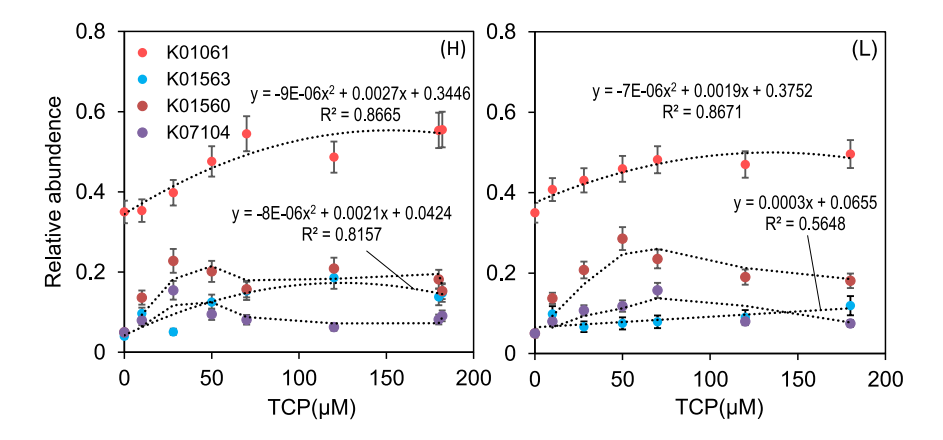


Fig. 5. Comparative analysis of alpha diversity index in early phases (a) and late phases (b).  $P < 0.001^{***}, 0.001 < P \le 0.01^{**}, 0.01 < P \le 0.05^{*}.$ 



**Fig. 6.** Correlation analysis between key genes and TCP concentration. R is the correlation coefficient, and is generally considered: when |R| > 0.7: strong correlation; 0.5 < |R| < 0.7: moderate correlation; 0.3 < |R| < 0.5: weak correlation; |R| < 0.3: no correlation.  $R^2 > 0.7$ 5 indicating excellent fit of the model and high interpretability. K01061: EC 3.1.1.45 gene; K01560: EC 3.8.1.2 gene; K07104: EC 1.3.11.2 gene; K01563: EC 3.8.1.5 gene.

analysis (Fig. 4), indicating that 70  $\mu M$  TCP represents a critical threshold.

As shown in Fig. 7a, EC 3.1.1.45, and EC 3.8.1.5, had higher abundances in H ( $\sim$ 55% and 26.5%, respectively) than in L ( $\sim$ 47% and 10.5%, respectively) (P < 0.05). EC 3.1.1.45 is associated with the cleavage of the cyclic structure. The high abundance and increasing trend for this gene were detected mainly from  $\delta$ -Proteobacteria, *Methanosarcina*, and *Methanoperedens* (Fig. 7b). Ring-opening genes have previously been detected in methanogens previously (Sandhu et al., 2022; Chen et al., 2016). Unclassified  $\delta$ -Proteobacteria (18.7%/35.2%, NR species abundance/functional contribution, the same hereinafter) in

H was the most dominant taxon annotated to EC 3.1.1.45. In L, the species annotated as EC 3.1.1.45 were mainly *Methanoperedens* (8.4%/17.6%), *Ardenticatena* (6.1%/11.5%), and *Methanosarcina* (4.7%/9.1%). EC 3.8.1.5 catalyzes hydrolytic cleavage (Chaloupkova et al., 2019). Hou et al. (2022) reported the removal of Cl from hexachloride using this enzyme. The species with the enzyme in both systems were consistent, namely, an unclassified Bacteria (genus), *Mycobacterium*, and *Hahella*, but the abundance and functional contribution in H (4.9%/26.1%, 2.7%/6.7%, and 3.0%/19.7%) were significantly higher (P < 0.05) than those in L (2.5%/10.5%, 0.8%/3.4%, and 0.3%/3.8%). The higher abundances of these two genes may explain the stronger

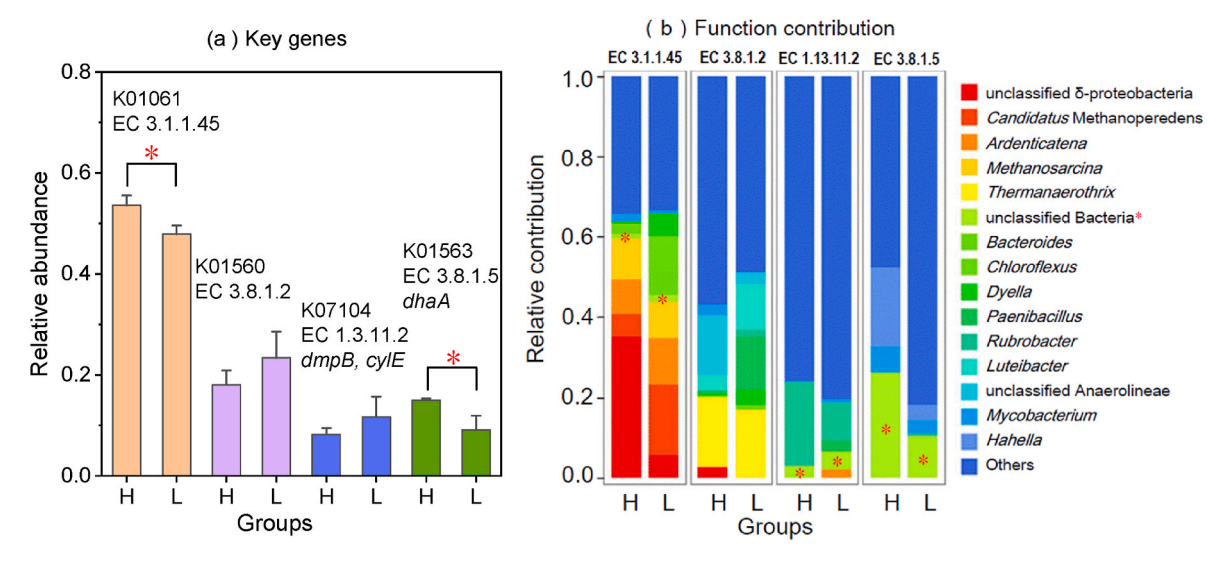


Fig. 7. (a) Relative abundances of key functional genes according to metagenome sequencing. The top 4 genes for abundance are shown. Red stars (\*) represent a significant difference (P < 0.05). (b) Functional contributions of enzymes. The top 5 enzyme functions and top 15 genera are shown. Red stars (\*) represent unclassified Bacteria.

dechlorination ability of the H system.

EC 3.8.1.2, which is considered the key enzyme for hydrolytic dechlorination, was highly abundant over time in both systems (no significant difference). This enzyme catalyzes the hydrolytic removal of chlorine. EC 3.8.1.2, in prokaryotes, can biotransform a wide spectrum of chlorinated compounds with high catalytic efficiency and chiral resolution (Adamu et al., 2017; Oyewusi et al., 2021). In H, EC 3.8.1.2 mainly clustered into two genera of the class Anaerolineae: *Thermanaerothrix* (3.1%/17.3%) and unclassified Anaerolineae (2.9%/15.1%). Anaerolineae is responsible for fermentation (Gregoire et al., 2011) but also performs dechlorination via the hydrolytic enzyme EC 3.8.1.2.

EC 1.13.11.2 converts the benzene ring of catechol into 2-hydroxyl mucilagaldehyde (Zeng et al., 2020), and this is a rate-limiting enzyme for aromatic ring degradation that reduces the harmful effects of catechol accumulation on bacterial cells (Zhang et al., 2022). The functional contributor of this enzyme was *Rubrobacter*, and its functional contribution to H (2.3%/20.9%) was twice (P < 0.05) that to L (1.7%/9.4%).

An unknown genus with multiple functions (dechlorinating (EC 3.8.1.5) and ring-opening (EC 3.1.1.45, EC 1.13.11.2)) and unclassified Bacteria (Fig. 7b, marked with\*, identified in Fig. 2b) had a higher (P < 0.05) abundance and contribution of EC 3.8.1.5 in H (4.9%/26.1%) than in L (2.5%/10.5%). This implies that this single bacterium may have been able to realize the completely degraded TCP, which is rare occurrence in nature (Saleem et al., 2019).

Overall, the ring-opening process, catalyzed by EC 3.1.1.45, is important for TCP-biodegrading is associated with the biodegradation of various halogenated aromatic hydrocarbons (Gaytan et al., 2020; Arora and Bae, 2014; Solyanikova et al., 2003). Hydrolytic dechlorination bacteria are related to the effectiveness of the system, similar to the non-respiratory dechlorination of chlorinated natural organic matter in uncontaminated anaerobic soils (Temme et al., 2019).

As shown in Fig. 8, while each group in H occupied a specific functional *niche*, they jointly performed the reactions required to completely biotransform TCP. Although RDases are not annotated here, reductive dechlorination was performed in the initial steps (green arrows) based on the detected products. Respiratory dechlorination is a common mechanism in anaerobic chlorine-contaminated environment (Adrenz and Loffler., 2016; Ni et al., 1995), and involves a variety of species. Annotated hydrolytic dehalogenases (EC 3.8.1.X) were present and likely responsible for some dechlorination. HLDs are widely distributed under aerobic condition (Bhattarai et al., 2022; Fetzner, 1998). The

common outcome of the reduction and hydrolytic enzyme activities is the removal of Cl atoms from the chain or cyclic organic backbone molecules, liberating carbon for common metabolic steps carried out by fermentation bacteria and, ultimately, methanogens. The evidence herein supports the idea that HLDs are important in anaerobic systems, as reductive and hydrolytic dechlorination jointly produce products that can serve as growth substrates for bacteria, as has been seen before (Temme et al., 2019; Adamu et al., 2017).

Due to sustained environmental pressure, microbial communities realign and "assemble" novel metabolic pathways. The pathways for TCP in Fig. 8 show how the H community adapted to simultaneously tolerate the high toxicity of TCP and ultimately biotransform TCP. The TCP  $\rightarrow$  4-CP step of H was more complete than that of L, indicating that H had a high functional level for reductive dechlorination. Key for the H community was EC 3.8.1.5, which catalyzes hydrolytic dechlorination, a nucleophilic substitution (Verschueren et al., 1993), and which has shown a positive correlation with temperature (35–50 °C) (Xi et al., 2015). This gene and its related microorganisms were clustered in H, strengthening the functionality and stability of the H community.

## 4. Conclusion

It was demonstrated that robust communities grew under some specific combinations of environmental factors, posing high collectivization, degree, and evenness. Core taxa include dechlorinators (unclassified Anaerolineae, *Thermanaerothrix* and *Desulfovibrio*), ringopening microorganisms (unclassified δ-Proteobacteria, *Methanosarcina*, *Methanoperedens*, and *Rubrobacter*) and dominant species of climax communities (Thermodesulfovibrionia, *Syntrophbacter*). We emphasized the significance of syntrophic bacteria especially for the deterministically ecological process—the expansion of *niches* under high temperatures. We also discovered a positive correlation between the abundance of genes involved in hydrolysis dechlorination and ringopening and TCP loading. The relevant microorganisms were annotated, whose metabolic pathways were simultaneously predicted.

The new findings provided some evidences to the engineering, regulation, and design of synthetic microbiomes, which would help understand the mechanisms, predictions, and operations of the collaborative biodegradation for various contaminants.

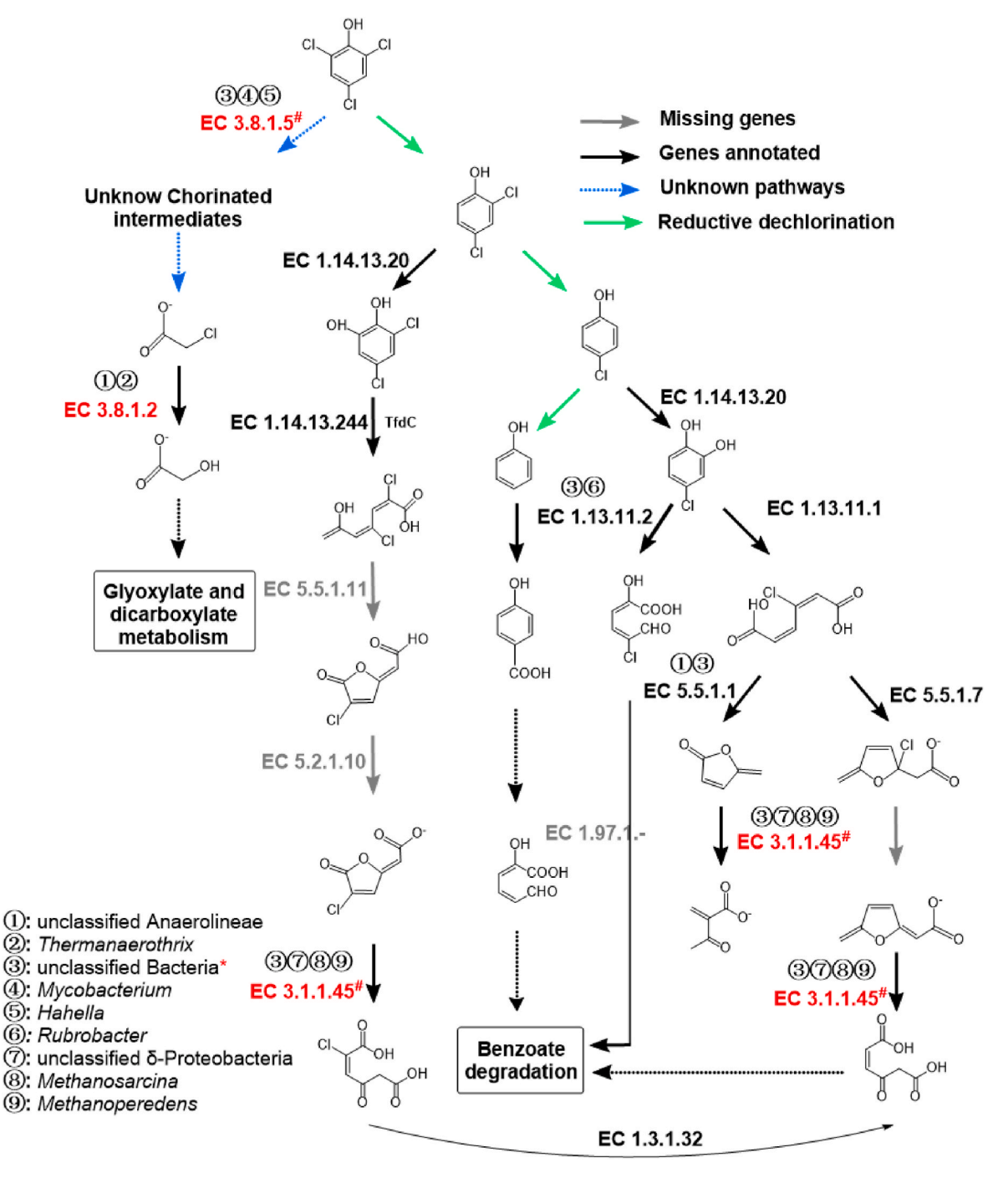


**Fig. 8.** Construction of chlorophenol metabolic pathways based on identified functional genes. Blue arrows indicate missing genes. Species contributing to the functional genes for core enzymes are listed next to the core enzymes. Symbol \* represents a core taxon with multiple functions. Symbol # means enzymes with significant differences in abundance between the groups.

# Credit author statement

Ming Lin: Project administration, Investigation, Writing – original draft, Formal analysis; Chenhui Pan: Project administration, Formal analysis, editing; Chenyi Qian: Investigation, Formal analysis; Fei Tang: Investigation; Siwen Zhao: Investigation; Jun Guo: Data curation, Formal analysis, Methodology; Yongming Zhang: review; Jiaxiu Song: Project administration, Methodology, Formal analysis, writing, review, editing, Validation, Supervision and funding acquisition; Bruce E. Rittmann: Conceptualization, Methodology, review and editing. All authors have read and consent to the final version of the manuscript.

# **Declaration of competing interest**

The authors declare that they have no known competing financial interests or personal relationships that could have appeared to influence the work reported in this paper.

# Data availability

Data will be made available on request.

#### Acknowledgements

This research was sponsored by the National Natural Science Foundation of China (No. 21677100); the Natural Science Foundation of Shanghai (23ZR1446900); and the Fundamental Research Funds for the Central Universities (No. B210204007) and PAPD.

### Appendix A. Supplementary data

Supplementary data to this article can be found online at https://doi.org/10.1016/j.envres.2023.117591.

### References

- Adamu, A., Wahab, R.A., Shamsir, M.S., Aliyu, F., Huyop, F., 2017. Deciphering the catalytic amino acid residues of L-2-haloacid dehalogenase (DehL) from rhizobium sp. RC1: an in silico analysis. Comput. Biol. Chem. 70, 125–132. https://doi.org/ 10.1016/j.compbiolchem.2017.08.007.
- Adrenz, L., Loffler, F.E., 2016. Organohalide-Respiring Bacteria. Spring-Verlag, GER.Adrian, L., Szewzyk, U., Wecke, J., Gorisch, H., 2000. Bacterial dehalorespiration with chlorinated benzenes. Nature 408, 580. https://doi.org/10.1038/35046063.
- Ali, S.S., Kornaros, M., Manni, A., Sun, J., El-Shanshoury, A.E.R., Kenawy, E., Khalil, M. A., 2020. Enhanced anaerobic digestion performance by two artificially constructed microbial consortia capable of woody biomass degradation and chlorophenols detoxification. J. Hazard Mater. 389, 122076 https://doi.org/10.1016/j.jhazmat.2020.122076.
- Anam, G.B., Choi, J., Ahn, Y., 2019. Reductive dechlorination of perchloroethene (PCE) and bacterial community changes in a continuous-flow, two-stage anaerobic column. Int. Biodeterior. Biodegrad. 138, 41–49. https://doi.org/10.1016/j.ibiod.2018.13.014.
- Arora, P.K., Bae, H., 2014. Bacterial degradation of chlorophenols and their derivatives. Microbial Microb. Cell Fact. 13, 1–17. https://doi.org/10.1186/1475-2859-13-31.
- Assadi, A., Alimoradzadeh, R., Movahedyan, H., Amin, M.M., 2021. Intensified 4-chlor-ophenol biodegradation in an aerobic sequencing batch reactor: microbial and kinetic properties evaluation. Environ. Technol. Inno. 21, 101243 https://doi.org/10.1016/j.eti.2020.101243.
- Bai, L., Liu, X., Hua, K., Tian, L., Wang, C., Jiang, H., 2022. Microbial processing of autochthonous organic matter controls the biodegradation of 17α-ethinylestradiol in lake sediments under anoxic conditions. Environ. Pollut. 296, 118760 https://doi. org/10.1016/j.envpol.2021.118760.
- Bhattarai, S., Temme, H., Jain, A., Badalamenti, J.P., Gralnick, J.A., Novak, P.J., 2022. The potential for bacteria from carbon-limited deep terrestrial environments to participate in chlorine cycling. Fems Microb. Ecol. 98 (6), 54. https://doi.org/ 10.1093/femsec/fjac054.
- Chaloupkova, R., Liskova, V., Toul, M., Markova, K., Sebestova, E., Hernychova, L., Marek, M., Pinto, G.P., Pluskal, D., Waterman, J., 2019. Light-emitting dehalogenases: reconstruction of multifunctional biocatalysts. ACS Catal. 9 (6), 4810–4823. https://doi.org/10.1021/acscatal.9b01031.
- Chattopadhyay, I., Usman, T.M., Varjani, S., 2022. Exploring the role of microbial biofilm for industrial effluents treatment. Bioengineered 13 (3), 6420–6440. https:// doi.org/10.1080/21655979.2022.2044250.
- Chen, Y., Black, D.S., Reilly, P.J., 2016. Carboxylic ester hydrolases: classification and database derived from their primary, secondary, and tertiary structures. Protein Sci. 25 (11), 1942–1953. https://doi.org/10.1002/pro.3016.
- Chen, G., Jiang, N., Solis, M.I.V., Murdoch, F.K., Murdoch, R.W., Xie, Y., Swift, C.M., Hettich, R.L., Loffler, F.E., 2021. Anaerobic microbial metabolism of dichloroacetate. mBio 12, e521–e537. https://doi.org/10.1128/mBio.00537-21.
- Chmelova, K., Sebestova, E., Liskova, V., Beier, A., Bednar, D., Prokop, Z., Chaloupkova, R., Damborsky, J., 2020. A haloalkane dehalogenase from saccharomonospora viridis strain DSM 43017, a compost bacterium with unusual catalytic residues, unique (S)-Enantiopreference, and high thermostability. AEM 86 (17), e02820. https://doi.org/10.1128/AEM.02820-19.
- Chovancova, E., Kosinski, J., Bujnicki, J.M., Damborsky, J., 2007. Phylogenetic analysis of haloalkane dehalogenases. Proteins 67 (2), 305–316. https://doi.org/10.1002/ prot.21313.
- Coskun, O.K., Ozen, V., Wankel, S.D., Orsi, W.D., 2019. Quantifying population-specific growth in benthic bacterial communities under low oxygen using H218O. ISME J. 13 (6), 1546–1559. https://doi.org/10.1038/s41396-019-0373-4.
- Delgado, A.G., Fajardo-Williams, D., Bondank, E., Esquivel-Elizondo, S., 2017. Krajmalnik-Brown, R. Coupling bioflocculation of dehalococcoides mccartyi to high-rate reductive dehalogenation of chlorinated ethenes. Environ. Sci. Technol. 51 (19), 11297–11307. https://doi.org/10.1021/acs.est.7b0309.
- Diaz-Baez, M.C., Valderrama-Rincon, J.D., 2017. Rapid restoration of methanogenesis in an acidified UASB reactor treating 2,4,6-trichlorophenol (TCP). J. Hazard Mater. 324, 599–604. https://doi.org/10.1016/j.jhazmat.2016.11.031.
- EPA, 2015. Priority Pollutant List. US Environmental Protection Agency, Washington, DC. https://www.epa.gov/sites/production/files/2015-09/documents/priority-poll utant-list-epa.pdf.
- Fetzner, S., 1998. Bacterial dehalogenation. J. Assoc. Music Imagery 50, 633–657. https://doi.org/10.1007/s002530051346.

- Gao, R., Wang, J., 2007. Effects of PH and temperature on isotherm parameters of chlorophenols biosorption to anaerobic granular sludge. J. Hazard Mater. 145 (3), 398–403. https://doi.org/10.1016/j.jhazmat.2006.11.036.
- Gaytan, I., Sanchez-Reyes, A., Burelo, M., Vargas-Suarez, M., Liachko, I., Press, M., Sullivan, S., Cruz-Gomez, M.J., Loza-Tavera, H., 2020. Degradation of recalcitrant polyurethane and xenobiotic additives by a selected landfill microbial community and its biodegradative potential revealed by proximity ligation-based metagenomic analysis. Front. Microbiol. 10, 2986. https://doi.org/10.3389/fmicb.2019.02986.
- Ghattas, A.K., Fischer, F., Wick, A., Ternes, T.A., 2017. Anaerobic biodegradation of (emerging) organic contaminants in the aquatic environment. Water Res. 116, 268–295. https://doi.org/10.1016/j.watres.2017.02.001.
- Gralka, M., Szabo, R., Stocker, R., Cordero, O.X., 2020. Trophic interactions and the drivers of microbial community assembly. Curr. Biol. 30 (19), R1176–R1188. https://doi.org/10.1016/j.cub.2020.08.007.
- Gregoire, P., Fardeau, M.L., Joseph, M., Guasco, S., Hamaide, F., Biasutti, S., Michotey, V., Bonin, P., Ollivier, B., 2011. Isolation and characterization of Thermanaerothrix daxensis gen. Nov., sp. Nov., a thermophilic anaerobic bacterium pertaining to the phylum "Chloroflexi". Isolated from a Deep Hot Aquifer in the Aquitaine Basin. Syst. Appl. Microbiol. 34 (7), 494–497. https://doi.org/10.1016/j. svaom.2011.02.004.
- Hasan, K., Fortova, A., Koudelakova, T., Chaloupkova, R., Ishitsuka, M., Nagata, Y., Damborsky, J., Prokop, Z., 2011. Biochemical characteristics of the novel haloalkane dehalogenase DatA, isolated from the plant pathogen agrobacterium tumefaciens CS8. AEM 77 (5), 1881–1884. https://doi.org/10.1128/AEM.02109-10.
- He, Z., Zhu, Y., Feng, J., Ji, Q., Chen, X., Pan, X., 2021. Long-term effects of four environment-related iron minerals on microbial anaerobic oxidation of methane in paddy soil: a previously overlooked role of widespread goethite. Soil. Boil. Biochem. 161, 108387 https://doi.org/10.1016/j.soilbio.2021.108387.
- Hou, J., Zhang, Y., Wu, X., Liu, L., Wu, Y., Liu, W., Christie, P., 2022. Zero-valent iron-induced successive chemical transformation and biodegradation of lindane in historically contaminated soil: an isotope-informed metagenomic study. J. Hazard Mater. 433, 128802 https://doi.org/10.1016/j.jhazmat.2022.128802.
- Hug, L.A., Beiko, R.G., Rowe, A.R., Richardson, R.E., Edwards, E.A., 2012. Comparative metagenomics of three dehalococcoides-containing enrichment cultures: the role of the non-dechlorinating community. BMC Genom. 13 (1), 327. https://doi.org/ 10.1186/1471-2164-13-327.
- Iasakov, T.R., Kanapatskiy, T.A., Toshchakov, S.V., Korzhenkov, A.A., Ulyanova, M.O., Pimenov, N.V., 2022. The baltic sea methane pockmark microbiome: the new insights into the patterns of relative abundance and ANME niche separation. Mar. Environ. Res. 173, 105533 https://doi.org/10.1016/j.marenvres.2021.105533.
- Jesenska, A., Monincova, M., Koudelakova, T., Hasan, K., Chaloupkova, R., Prokop, Z., Geerlof, A., Damborsky, J., 2009. Biochemical characterization of haloalkane dehalogenases DrbA and DmbC, representatives of a novel subfamily. AEM 75 (15), 5157–5160. https://doi.org/10.1128/AEM.00199-09.
- Jugder, B., Ertan, H., Bohl, S., Lee, M., Marquis, C.P., 2016. Manefield, M. Organohalide respiring bacteria and reductive dehalogenases: key tools in organohalide bioremediation. Front. Microbiol. 7 https://doi.org/10.3389/fmicb.2016.00249.
- Juteau, P., Beaudet, R., McSween, G., Lepine, F., Milot, S., Bisaillon, J.G., 1995.
  Anaerobic biodegradation of pentachlorophenol by a methanogenic consortium.
  Appl. Microbiol. Biotechnol. 44 (1), 218–224. https://doi.org/10.1007/BF00164505.
- Kapoor, R.T., Salvadori, M.R., Rafatullah, M., Siddiqui, M.R., Khan, M.A., Alshareef, S.A., 2021. Exploration of microbial factories for synthesis of nanoparticles–a sustainable approach for bioremediation of environmental contaminants. Front. Microbiol. 12, 658294 https://doi.org/10.3389/fmicb.2021.658294.
- Kaya, D., Kjellerup, B.V., Chourey, K., Hettich, R.L., Taggart, D.M., Loffler, F.E., 2019. Impact of fixed nitrogen availability on dehalococcoides mccartyi reductive dechlorination activity. Environ. Sci. Technol. 53 (24), 14548–14558. https://doi. org/10.1021/acs.est.9b04463.
- Konovalova, E.I., Solyanikova, I.P., Golovleva, L.A., 2009. Degradation of 4-chlorophenol by the strain rhodococcus opacus 6a. Microbiology 78 (6), 805–807. https://doi.org/10.1134/S0026261709060204.
- Kravos, A., Zgajnar Gotvajn, A., Lavrencic Stangar, U., Malinovic, B.N., Prosen, H., 2022. Combined analytical study on chemical transformations and detoxification of model phenolic pollutants during various advanced oxidation treatment processes. Molecules 27 (6), 1935. https://doi.org/10.3390/molecules27061935.
- Kruse, S., Turkowsky, D., Birkigi, J., Matturro, B., Franke, S., Jehmlich, N., Von Bergen, M., Westermann, M., Rossetti, S., Nijenhuis, I., Adrian, L., Diekert, G., Goris, T., 2021. Interspecies metabolite transfer and aggregate formation in a Coculture of dehalococcoides and sulfurospirillum dehalogenating tetrachloroethene to ethene. ISME J. 15 (6), 1794–1809. https://doi.org/10.1038/s41396-020-00887-6.
- Kulikova, N.A., Perminova, I.V., 2021. Interactions between humic substances and microorganisms and their implications for nature-like bioremediation technologies. Molecules 26 (9), 2706. https://doi.org/10.3390/molecules26092706.
- Li, A., Shao, Z., 2014. Biochemical characterization of a haloalkane dehalogenase DadB from alcanivorax dieselolei B-5. PLoS One 9 (2), e89144. https://doi.org/10.1371/ journal.pone.0089144.
- Li, Y., Sun, Y., Li, L., Yuan, Z., 2018. Acclimation of acid-tolerant methanogenic propionate-utilizing culture and microbial community dissecting. Bioresour. Technol. 250, 117–123. https://doi.org/10.1016/j.biortech.2017.11.034.
- Li, Y., Wen, L.L., Zhao, H.P., Zhu, L., 2019. Addition of shewanella oneidensis MR-1 to the dehalococcoides-containing culture enhances the trichloroethene dechlorination. Envrion. Int. 133, 105245 https://doi.org/10.1016/j.envint.2019.105245.
- Limam, I., Limam, R.D., Mezni, M., Guenne, A., Madigou, C., Driss, M.R., Bouchez, T., Mazeas, L., 2016. Penta- and 2,4,6-tri-chlorophenol biodegradation during

- municipal solid waste anaerobic digestion. Ecotox. Environ. Safe. 130, 270–278. https://doi.org/10.1016/i.ecoeny.2016.04.030.
- Lin, X., Li, Z., Liang, B., Zhai, H., Cai, W., Nan, J., Wang, A., 2019. Accelerated microbial reductive dechlorination of 2,4,6-trichlorophenol by weak electrical stimulation. Water Res. 162, 236–245. https://doi.org/10.1016/j.watres.2019.06.068.
- Lucas, D., Petty, S.M., Keen, O., Luedeka, B., Schlummer, M., Weber, R., Yazdani, R., Riise, B., Rhodes, J., Nightingale, D., Diamond, M.L., Vijgen, J., Lindeman, A., Blum, A., Koshland, C.P., 2018. Methods of responsibly managing end-of-life foams and plastics containing flame retardants: Part II. Environ. Eng. Sci. 35, 588–602. https://doi.org/10.1089/ees.2017.0380.
- Mai, D.T., Stuckey, D.C., 2018. Oh, effect of ciprofloxacin on methane production and anaerobic microbial community. Bioresour. Technol. 261, 240–248. https://doi.org/ 10.1016/j.biortech.2018.04.009.
- Matturro, B., Ubaldi, C., Rossetti, S., 2016. Microbiome dynamics of a polychlorobiphenyl (PCB) historically contaminated marine sediment under conditions promoting reductive dechlorination. Front. Microbiol. 7, 1502. https:// doi.org/10.3389/fmicb.2016.01502.
- Mikesell, M.D., Boyd, S.A., 1986. Complete reductive dechlorination and mineralization of pentachlorophenol by anaerobic microorganisms. AEM 52 (4), 861–865. https:// doi.org/10.1128/aem.52.4.861-865.1986.
- Mortan, S.H., Martin-Gonzalez, L., Vicent, T., Caminal, G., Nijenhuis, I., Adrian, L., Marco-Urrea, E., 2017. Detoxification of 1,1,2-trichloroethane to ethene in a bioreactor Co-culture of dehalogenimonas and dehalococcoides mccartyi strains. J. Hazard Mater. 331, 218–225. https://doi.org/10.1016/j.jhazmat.2017.02.043.
- Ni, S., Fredrickson, J.K., Xun, L., 1995. Purification and characterization of a novel 3-chlorobenzoate-reductive dehalogenase from the cytoplasmic membrane of desulfomonile tiedjei DCB-1. J. Bacteriol. 177 (17), 5135–5139. https://doi.org/10.1128/jb.177.17.5135-5139.1995.
- Nordin, K., Unell, M., Jansson, J.K., 2005. Novel 4-chlorophenol degradation gene cluster and degradation route via hydroxyquinol in arthrobacter chlorophenolicus A6. AEM 71 (11), 6538–6544. https://doi.org/10.1128/AEM.71.11.6538-6544.2005
- Oyewusi, H.A., Huyop, F., Wahab, R.A., 2021. Genomic characterization of a dehalogenase-producing bacterium (Bacillus megaterium H2) isolated from hypersaline lake tuz (Turkey). Gene Reports 25, 101381. https://doi.org/10.1016/j.genrep.2021.101381.
- Patel, N., Shahane, S., Bhunia, B., Mishra, U., Chaudhary, V.K., 2022. Srivastav, A.L. Biodegradation of 4-chlorophenol in batch and continuous packed bed reactor by isolated Bacillus subtilis. JEM 301, 113851. https://doi.org/10.1016/j.jenvman.2021.113851.
- Payne, R.B., Ghosh, U., May, H.D., Marshall, C.W., Sowers, K.R., 2019. A pilot-scale field study: in situ treatment of PCB-impacted sediments with bioamended activated carbon. Environ. Sci. Technol. 53 (5), 2626–2634. https://doi.org/10.1021/acs. est.8b05019.
- Qi, M., Liang, B., Zhang, L., Ma, X., Yan, L., Dong, W., Kong, D., Zhang, L., Zhu, H., Gao, S.H., Jiang, J., Liu, S.J., Corvini, P.F., Wang, A., 2021. Microbial interactions drive the complete catabolism of the antibiotic sulfamethoxazole in activated sludge microbiomes. Environ. Sci. Technol. 55 (5), 3270–3282. https://doi.org/10.1021/ page 10.0000000.
- Ren, Y., Yu, G., Shi, C., Liu, L., Guo, Q., Han, C., Zhang, D., Zhang, L., Liu, B., Gao, H., 2022. Majorbio Cloud: a one-stop, comprehensive bioinformatic platform for multiomics analyses. Imeta 1 (2), e12. https://doi.org/10.1002/imt2.12.
- Rittmann, B.E., McCarty, P.L., 2012. Environmental Biotechnology: Principles and AppliWacations. Oinghua University Press, CHN (Chinese).
- Saleem, M., Hu, J., Jousset, A., 2019. More than the sum of its parts: microbiome biodiversity as a driver of plant growth and soil health. Annu. Rev. Ecol. Evol. S 50, 145–168. https://doi.org/10.1146/annurev-ecolsys-110617-062605.
- Sandhu, M., Paul, A.T., Jha, P.N., 2022. Metagenomic analysis for taxonomic and functional potential of polyaromatic hydrocarbons (PAHs) and polychlorinated biphenyl (PCB) degrading bacterial communities in steel industrial soil. PLoS One 17 (4), e0266808. https://doi.org/10.1371/journal.pone.0266808.
- Semenova, E.M., Babich, T.L., Sokolova, D.S., Ershov, A.P., Raievska, Y.I., Bidzhieva, S. K., Stepanov, A.L., Korneykova, M.V., Myazin, V.A., Nazina, T.N., 2022. Microbial communities of seawater and coastal soil of Russian arctic region and their potential for bioremediation from hydrocarbon pollutants. Microorganisms 10 (8), 1490. https://doi.org/10.3390/microorganisms10081490.
- Singh, D.P., Prabha, R., Gupta, V.K., Verma, M.K., 2018. Metatranscriptome analysis deciphers multifunctional genes and enzymes linked with the degradation of aromatic compounds and pesticides in the wheat rhizosphere. Front. Microbiol. 9, 1331. https://doi.org/10.3389/fmicb.2018.01331.

- Solyanikova, I.P., Golovleva, L.A., 2004. Bacterial degradation of chlorophenols: pathways, biochemica, and genetic aspects. J. Environ. Sci. Health. B 39, 333–351. https://doi.org/10.1081/pfc-120035921.
- Solyanikova, I.P., Golovleva, L.A., 2011. Biochemical features of the degradation of pollutants by rhodococcus as a basis for contaminated wastewater and soil cleanup. Microbiol. 80 (5), 591–607. https://doi.org/10.1134/S0026261711050158.
- Solyanikova, I.P., Moiseeva, O.V., Boeren, S., Boersma, M.G., Kolomytseva, M.P., Vervoort, J., Rietjens, I.M., Golovleva, L.A., van Berkel, W.J., 2003. Conversion of 2fluoromuconate to cis-dienelactone by purified enzymes of rhodococcus opacus 1cp. AEM 69 (9), 5636–5642. https://doi.org/10.1128/AEM.69.9.5636-5642.2003.
- Song, J., Zhao, Q., Guo, J., Yan, N., Chen, H., Sheng, F., Lin, Y., An, D., 2019. The microbial community responsible for dechlorination and benzene ring opening during anaerobic degradation of 2,4,6-trichlorophenol. Sci. Total Environ. 651, 1368–1376. https://doi.org/10.1016/j.scitotenv.2018.09.300.
- Sun, C., Zhang, B., Ning, D., Zhang, Y., Dai, T., Wu, L., Li, T., Liu, W., Zhou, J., Wen, X., 2021. Seasonal dynamics of the microbial community in two full-scale wastewater treatment plants: diversity, composition, phylogenetic group based assembly and Cooccurrence pattern. Water Res. 200, 117295 https://doi.org/10.1016/j. watres 2021 117295
- Temme, H.R., Carlson, A., Novak, P.J., 2019. Presence, diversity, and enrichment of respiratory reductive dehalogenase and non-respiratory hydrolytic and oxidative dehalogenase genes in terrestrial environments. Front. Microbiol. 10, 01258 https:// doi.org/10.3389/fmicb.2019.01258.
- Vanwonterghem, I., Jensen, P.D., Rabaey, K., Tyson, G.W., 2016. Genome-centric resolution of microbial diversity, metabolism and interactions in anaerobic digestion. Envrion. Microbiol. 18 (9), 3144–3158. https://doi.org/10.1111/1462-2920.13382.
- Verschueren, K.H., Seljée, F., Rozeboom, H.J., Kalk, K.H., Dijkstra, B.W., 1993.
  Crystallographic analysis of the catalytic mechanism of haloalkane dehalogenase.
  Nature 363 (6431), 693–698. https://doi.org/10.1038/363693a0.
- Wang, T., Zhu, G., Kuang, B., Jia, J., Liu, C., Cai, G., Li, C., 2021. Novel insights into the anaerobic digestion of propionate via syntrophobacter fumaroxidans and geobacter sulfurreducens: process and mechanism. Water Res. 200, 117270 https://doi.org/ 10.1016/j.watres.2021.117270.
- Watts, D.J., Strogatz, S.H., 1998. Collective dynamics of 'small-World' Networks. Nature 393 (6684), 440–442. https://doi.org/10.1038/30918.
- Wu, Y., Wu, J., Wu, Z., Zhou, J., Zhou, L., Lu, Y., Liu, X., Wu, W., 2021. Groundwater contaminated with short-chain chlorinated paraffins and microbial responses. Water Res. 204, 117605 https://doi.org/10.1016/j.watres.2021.117605.
- Xi, H., Liu, C., Wen, X., Chen, L., 2015. Advances in research on haloalkane dehalogenases and its sulfur mustard degradation function. Chin. J. Appl. Environ. Biol. 21 (5), 842–847.
- Yan, J., Wang, J., Villalobos Solis, M.I., Jin, H., Chourey, K., Li, X., Yang, Y., Yin, Y., Hettich, R.L., Loffler, F.E., 2021. Respiratory vinyl chloride reductive dechlorination to ethene in TceA-expressing dehalococcoides mccartyi. Environ. Sci. Technol. 55 (8), 4831–4841. https://doi.org/10.1021/acs.est.0c07354.
- Yang, J., Speece, R.E., 1986. The effects of chloroform toxicity on methane formation. Water Res. 20, 1273–1279. https://doi.org/10.1016/0043-1354(86)90158-2.
- Yang, Y., Sanford, R., Yan, J., Chen, G., Capiro, N.L., Li, X., Loffler, F.E., 2020. Roles of organohalide-respiring Dehalococcoidia in carbon cycling. mSystems 5 (3), 1–12. https://doi.org/10.1128/mSystems.00757-19.
- Yu, J., Tang, S.N., Lee, P.K., 2021. Microbial communities in full-scale wastewater treatment systems exhibit deterministic assembly processes and functional dependency over time. Environ. Sci. Technol. 55 (8), 5312–5323. https://doi.org/ 10.1021/acs.est.0c06732.
- Zeng, X.H., Du, H., Zhao, H.M., Xiang, L., Feng, N.X., Li, H., Li, Y.W., Cai, Q.Y., Mo, C.H., Wong, M.H., 2020. Insights into the binding interaction of substrate with catechol 2, 3-dioxygenase from biophysics point of view. J. Hazard Mater. 391, 122211 https://doi.org/10.1016/j.jhazmat.2020.122211.
- Zerva, I., Remmas, N., Kagalou, I., Melidis, P., Ariantsi, M., Sylaios, G., Ntougias, S., 2021. Effect of chlorination on microbiological quality of effluent of a full-scale wastewater treatment plant. Life Sci. 11 (1), 68. https://doi.org/10.3390/ life11010068.
- Zhang, H., Wu, J., Li, R., Kim, D.H., Bi, X., Zhang, G., Jiang, B., Ng, H.Y., Shi, X., 2022. Novel intertidal wetland sediment-inoculated moving bed biofilm reactor treating high-salinity wastewater: metagenomic sequencing revealing key functional microorganisms. Bioresour. Technol. 348, 126817 https://doi.org/10.1016/j. biortech.2022.126817.
- Zheng, S., Li, M., Liu, Y., Liu, F., 2021. Desulfovibrio feeding methanobacterium with electrons in conductive methanogenic aggregates from coastal zones. Water Res. 202, 117490 https://doi.org/10.1016/j.watres.2021.117490.